Middle-East Journal of Scientific Research 13 (10): 1419-1430, 2013
ISSN 1990-9233

DOI: 10.5829/idosi.mejsr.2013.13.10.1311

Modeling and Simulation of Mass Transfer in Tubular Gas-Liquid Membrane Contactors for Turbulent Flow Conditions and Comparison of Results with Laminar Flow Conditions

[1]N. Bakhshali, [2]R. Tahery and [3]H. Banazadeh

[1]Department of Chemical Engineering, Quchan Islamic Azad University, Quchan, Iran
[2]Department of Chemical Engineering, Islamic Azad University,
Tehran Central Branch, P.O. Box: 1469669191, Tehran, Iran
[3]Department of Chemical Engineering, Faculty of Engineering,
Ferdowsi University of Mashhad, Mashhad, Iran

Abstract: This Study mainly deals with modeling and simulation of turbulent flow conditions in gas absorption by liquid phase in a membrane contactor using computational fluid dynamics (CFD). For this purpose, single tube membrane contactor has been considered. The model has been based on "non-wetted mode", in which the gas mixture has filled membrane pores, for countercurrent gas-liquid contact. Axial and radial diffusion inside the tube, through the membrane and within the shell side of the membrane contactor have been considered. The simulation results have been compared with those of CO_2 absorption in water with laminar flow and similar physical conditions. Both predictions are in qualitative agreement with each other. However, the removal efficiency in turbulent flow conditions is much more than that of laminar flow conditions. It is also indicated that CO_2 removal from gas mixture is decreased with increasing gas volumetric flow rate. On the other hand, increasing liquid volumetric flow rate increases the removal efficiency.

Key words: Mass transfer · Membrane contactor · Turbulent flow · Modeling · Simulation

INTRODUCTION

A membrane contactor is a device that provides gas/liquid or liquid/liquid or gas/gas mass transfer without dispersion of one phase within another. This is accomplished by passing the fluids from opposite sides of a micro porous membrane. By careful control of the pressure difference between the fluids, one of the fluids entraps in the membrane pores resulting in, fluid/fluid interface at stagnant condition in each pore. This approach offers a number of important advantages over conventional dispersed phase contactors, including absence of emulsions, no flooding at high flow rates, no unloading at low flow rates, no density difference between fluids required and surprisingly high interfacial area. Indeed, membrane contactors typically offer 30 times more area than what is achievable in gas absorbers and 500 times what is obtainable in liquid/liquid extraction columns. Membrane contactor technology has been demonstrated in a range of liquid/liquid and gas/liquid applications in fermentation, pharmaceuticals, wastewater treatment, semiconductor manufacturing, carbonation of beverages, metal ion extraction, protein extraction and osmotic distillation [1].

Through the use of membrane contactors, membrane gas absorption process offers several economical advantages over conventional gas absorber column including: low investment costs, low pumping power and moreover, expensive civil engineering work is no more necessary [2]. Consequently, membrane gas absorption has been considered to be a promising and potentially large-scale application technology for gas separation processes.

Recently, membrane contactors have attracted many attentions as a new type process of gas absorption and much work has been done to study modeling and simulation of mass transfer in membrane contactors especially hollow fiber membrane (HFM) contactors for laminar conditions.

Corresponding Author: R. Tahery, Department of Chemical Engineering, Islamic Azad University,
Tehran Central Branch, P.O. Box: 1469669191, Tehran, Iran.

In order to gain a better understanding of CO_2 absorption in a HFM contactor, Hong-Yan Zhang *et al*. performed theoretical simulations to describe CO_2 capture by distilled water and aqueous diethanolamine (DEA) solutions. Their corresponding experiments were also carried out to verify the simulated results. In the case of physical absorption, both simulation and experimental results indicated that CO_2 flux was increased with increasing the liquid velocity, while the inlet gas velocity had no significant effect on CO_2 flux. In the case of chemical absorption, the CO_2 flux was significantly influenced by the inlet gas velocity while the liquid velocity had a limited effect [3].

A comprehensive two-dimensional mathematical model was developed by Al-Marzughi *et al*. for the transport of CO_2 through HFM contactors. They validated the model with the experimental results obtained for CO_2 removal from CO_2/CH_4 gas mixture using polypropylene (PP) membrane contactor with distilled water as the liquid solvent for different values of gas and liquid flow rate, gas to liquid ratio and temperature. Their simulation results indicated that the removal of CO_2 was increased with increasing liquid flow rate and decreasing gas flow rate [4]. In order to validate more the model, they also used the experimental data obtained using monoethanolamine (MEA) and sodium hydroxide (NaOH) solutions as solvents for CO_2 removal from CO_2/CH_4 gas mixture in PP HFM contactor. Both their simulation and experimental results indicated similar trends with previous ones [5].

Keshavarz *et al*. presented a mathematical model for a microporous HFM contactor operated under non-wet or partially wetted conditions, in order to analyze the simultaneous absorption of CO_2 and H_2S into an aqueous solution of DEA. Their results indicated that the membrane contactor can sequestrate both sour gases very effectively. Membrane wetting decreased the removal efficiency of both gases significantly in high wetting fractions. However, it mainly affected the CO_2 recovery in low wettings. The effects of various parameters on H_2S selectivity were investigated and it was found that the wetting of the membrane in low fractions increased the selectivity considerably. However, it had the opposite influence in high wetting fractions [6]. They also presented another mathematical model for gas absorption in microporous HFM contactors by using a random distribution of fibers. The chemical absorption of CO_2 into aqueous amine solutions and sulfur dioxide into water were simulated by this model. The model results were compared with four sets of different experimental data in the literature. The results indicated that the channeling of gas in the shell side decreased the efficiency of contactor significantly. It was found that the random distribution of fibers was a suitable method to simulate the commercial contactors [7].

Shirazian *et al*. presented the numerical simulation of momentum and mass transfer in a HFM contactor for laminar flow conditions using computational fluid dynamics (CFD). Their simulation results were compared with the experimental data obtained from literature for CO_2 absorption in pure water. The simulation results indicated that the removal of CO_2 was increased with increasing liquid flow rate in the shell side. On the other hand, increasing temperature and gas flow rate in the tube side had an opposite effect [8].

Mohebi *et al*. presented a numerical simulation using computational methods for sour gas sweetening. The HFM contactor and amine solution were used for separation of CO_2 and H_2S from $CO_2/H_2S/CH_4$ gas mixture. Sour gas and amine solution entered the shell and fiber, respectively. CO_2 and H_2S reacted with the amine solution. The results showed that concentrations of CO_2 and H_2S decreased in the beginning of the fiber. Liquid phase was controlling phase. Furthermore, pressure increase had a positive effect on separation [9].

Faiz and Al-Marzughi developed a comprehensive mathematical model for the simultaneous transport of CO_2 and H_2S through HFM contactors while using MEA as chemical solvent. Their model considered non-wetting and partial wetting conditions for countercurrent gas-liquid flow arrangement. The model results were in excellent agreement with experimental data for the physical absorption while considering non-wetting conditions. However, for chemical absorption the model showed excellent agreement with the experimental data while considering 10% wetting for PP membrane when 0.005M MEA was used and 50% wetting for polyvinyllidene fluoride (PVDF) membrane when 2M MEA was used [10]. They also considered the reaction mechanism of H_2S absorption into aqueous carbonate solution to be complicated due to the various species involved in the reaction. The previously developed comprehensive mathematical model was modified to account for the reversible reactions of all species involved in the chemical absorption of H_2S in aqueous carbonate solution using HFM contactors. The model predictions agreed well with experimental data provided from the literature for 2M carbonate solution under non-wetting conditions [11].

Sohrabi *et al*. studied chemical absorption of CO_2 theoretically using HFM contactors. They developed a mathematical model to study CO_2 transport through hollow-fiber membrane contactors. Their model predictions were validated with the experimental data obtained from literature for CO_2 absorption in amine aqueous solutions as solvent for different values of gas and liquid velocities. The liquid solvents considered for this study included aqueous solutions of MEA, DEA, N-methyldiethanolamine (MDEA), 2-amino-2-methyl-1-propanol (AMP) and potassium carbonate (K_2CO_3). Their simulation results indicated that amine aqueous solutions were better than K_2CO_3 aqueous solution for CO_2 absorption. Also the simulation results revealed that the removal of CO_2 with aqueous solution of MEA is the highest among the amine solvents [12].

El-Naas *et al*. assessed physical and chemical absorption of CO_2 into three different solvents through experimental investigation and mathematical modeling. A polypropylene HFM contactor was utilized to removal of CO_2 from a binary mixture containing 10% CO_2 in methane. They developed a mathematical model to characterize the effect of liquid and gas flow rates on membrane wettability and on the removal of CO_2. Their model considered complete wetting, partial wetting and non-wetting conditions. Both simulation and experimental results indicated that membrane wettability depended mostly on gas and solvent flow rates [13].

The absorption of carbon dioxide from nitrogen-carbon dioxide mixture was investigated in a polytetrafluoroethylene (PTFE) hollow fiber membrane module using potassium glycinate (PG) aqueous solution by Eslami *et al*. [14]. A mathematical model was developed to simulate the behavior of CO_2 removal by PG solution in hollow fiber module and solved for the non-wetted operation mode. The simulation results showed that both CO_2 mass transfer rate and removal efficiency were favored by concentration of PG, liquid flow rate and liquid temperature. Comparison of different diameters for the fibers of contactor and also different number of fibers showed that there is conditions of number and diameter of fibers which results in highest removal efficiency.

Some membrane systems normally operate under turbulent flow conditions [15]. But regretfully few researches have been done about momentum and mass transfer in membrane modules and contactors for turbulent flow conditions. Turbulent transport in a typical membrane module by CFD simulation was studied by Pellerin in 1994 [16]. A numerical hydrodynamic simulation of the flow field inside a membrane module has been formulated and implemented by them using finite difference method for solution of nonlinear differential equations for a finite number of nodes. A $k-\varepsilon$ model was used for turbulent flow conditions and a numerical procedure was run for a 25*36 grid. The velocity profiles and outlet concentration profile were predicted.

Predominant flow regime in hollow fiber and tubular membranes are laminar and turbulent, respectively. Surface area to volume ratio in hollow fiber membrane modules and contactors is more than it of tubular ones [15]. Thus it is interesting to investigate positive effect of turbulent flow conditions in comparison with laminar flow conditions on the removal and separation efficiency in a tubular membrane contactor containing a non-wetted membrane using modeling and simulation for compensating negative effect of its lower surface area to volume ratio. For this purpose, in present work, turbulent flow condition with pretty low Reynolds number is used for the modeling and simulation of physical absorption of CO_2 in a tubular membrane contactor with polytetrafluoroethylene (PTFE) membrane and compared with corresponding laminar flow condition for calculating the removal efficiency difference in two flow regimes.

Model Developments: In this paper, only physical absorption for non-wetting condition is considered. The effects of diffusion and convection on the removal rate are studied for CO_2-water system as case study. CH_4 transfer through the membrane and its absorption in water are neglected in comparison with these of CO_2.

Material Balance: A material balance has been carried out on a membrane contactor system to develop the main equations for the mathematical model. The model is developed for a single tube, as shown in Fig. 1, through which a solvent flows with a fully developed velocity profile. The fiber is surrounded by a laminar gas flow in an opposite d irection. Therefore, the membrane contactor consists of three sections: tube side, microporous membrane and shell side. The steady state two-dimensional material balances are carried out for all three sections. The gas mixture is fed to the shell side (at $Z = 0$), while the solvent is passed through the tube side (at $Z = L$). Carbon dioxide is removed from the mixture by diffusion through the membrane and then absorption in the solvent.

Shell Side: The steady state continuity equation for each species during the simultaneous mass transfer and chemical reaction in a reactive absorption system can be expressed as:

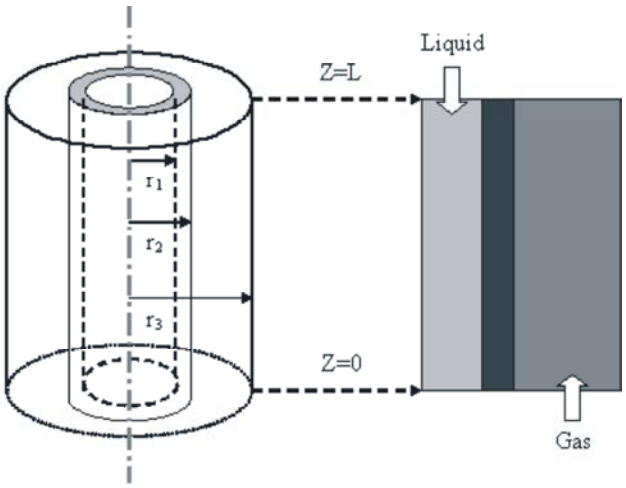

Fig. 1: Schematic diagram of the membrane contactor

$$-\nabla N_i \pm R_i = V_Z \frac{\partial C_i}{\partial z} \tag{1}$$

where C_i, N_i, R_i, V_z and z are the concentration, flux, reaction rate of species i, velocity and distance along the length of the membrane, respectively. Either Fick's law of diffusion or Maxwell-Stefan theory can be used for the determination of fluxes of species i. The overall rate of reaction of species i can be determined depending on the reaction mechanism and rates. The left-hand side of the above equations represents the diffusion and reaction terms, whereas the right hand side of the equation is the convection term. The differential equation for CO_2 in membrane contactors for cylindrical coordinate and no reaction condition is obtained using Fick's law of diffusion for the estimation of the diffusive flux:

$$D_{CO_2-shell}\left[\frac{\partial^2 C_{CO_2-shell}}{\partial r^2}+\frac{1}{r}\frac{\partial C_{CO_2-shell}}{\partial r}+\frac{\partial^2 C_{CO_2-shell}}{\partial z^2}\right]=V_{z-shell}\frac{\partial C_{CO_2-shell}}{\partial z} \tag{2}$$

where $D_{CO2-Shell}$ and r are the diffusion coefficient for CO_2 in shell side and radius, respectively.

Assuming H. Lamb model [17], the velocity profile in the shell is given by:

$$V_{z-shell}=2\langle V\rangle\left[1-(\frac{r}{r_3})^2-\frac{1-k^2}{Ln(1/k)}Ln(\frac{r_3}{r})\right] \tag{3}$$

where $\langle V\rangle$ is the mean velocity, k is the ratio of r_2 to r_3, r_2 is the outer radius of tube and r_3 is the inner radius of shell. The boundary conditions are given as:

$$z=0 \quad C_{CO_2-shell}=C_0 \tag{4}$$

$$r=r_3 \quad \frac{\partial C_{CO_2-shell}}{\partial r}=0 \tag{5}$$

$$r=r_2 \quad C_{CO_2-shell}=C_{CO_2-membrane} \tag{6}$$

$$z=L, \ N_{CO_2-shell}=C_{CO_2-shell}V_{z-shell} \ \text{(convective flux)} \tag{7}$$

where L is the contactor length.

Membrane: The steady-state material balance for the transport of CO_2 inside the membrane, which is considered to be due to diffusion alone, may be written as:

$$D_{CO_2-membrane}\left[\frac{\partial^2 C_{CO_2-membrane}}{\partial r^2}+\frac{1}{r}\frac{\partial C_{CO_2-membrane}}{\partial r}+\frac{\partial^2 C_{CO_2-membrane}}{\partial z^2}\right]=0 \quad (8)$$

The boundary conditions are given as:

$$r=r_1 \quad C_{CO_2-membrane}=\frac{C_{CO_2-tube}}{m} \quad (9)$$

$$r=r_2 \quad C_{CO_2-membrane}=C_{CO_2-Shell} \quad (10)$$

$$Z=0 \text{ and } Z=L \quad \nabla C_{CO2-membrane}=\text{(insulation)} \quad (11)$$

where m is the dimensionless Henry constant or physical solubility of CO_2 in the absorbent and r_1 is the inner radius of tube [5].

Tube Side: The steady state material balance for the transport of CO_2 in the tube side, where the gas mixture flows may be written as:

$$(D_{CO_2-tube}+D_{CO_2,turbulent-tube})\times\left[\frac{\partial^2 C_{CO_2-tube}}{\partial r^2}+\frac{1}{r}\frac{\partial C_{CO_2-tube}}{\partial r}+\frac{\partial^2 C_{CO_2-tube}}{\partial z^2}\right]=V_{z-tube}\frac{\partial C_{CO_2-tube}}{\partial z} \quad (12)$$

where:

$$D_{CO_2,turbulent-tube}=\frac{\nu^T}{Sc_{CO_2}{}^T} \quad (13)$$

where $Sc_{CO_2}{}^T$ is the turbulent Schmidt number for water-CO_2 solution and ν^T is the turbulent dynamic viscosity for water-CO_2 solution. The value or equation of these two parameters and the relevant parameters is listed in Table 1.

Where in Table 1, v^* is the fractional velocity, V is the mean velocity of liquid, τ_0 is the shear stress at the wall for turbulent flow, ρ is the fluid density and λ is the frictional resistance in smooth tubes. D is the inner diameter of tube and ν is the kinematics viscosity of liquid.

The velocity distribution in the tube side is assumed to follow Newtonian turbulent flow [17]:

$$V_{z-tube}=\frac{5}{4}V\left[1-(\frac{r}{r_1})\right]^{1/6} \quad (14)$$

where V is the average velocity in the tube side.
The boundary conditions are as follows:

$$z=L \quad C_{CO_2-tube}=0 \quad (15)$$

$$r=0 \quad \frac{\partial C_{CO2-tube}}{\partial r}=0 \quad (16)$$

$$r=r_1 \quad C_{CO2-tube}=C_{CO2-membrane}\times m \quad (17)$$

$$z=0 \quad N_{CO2-tube}=C_{CO2-tube}V_{z-tube} \text{ (convective flux)} \quad (18)$$

Table 1: Value or equation of necessary parameters

Parameter	Value or equation	Reference
$Sc_{CO_2}{}^T$	650	[18, 19]
ν^T (m²/s)	$0.08v^*r_1$	[20]
v^* (m/s)	$\mathrm{Re}\sqrt{\frac{\tau_0}{\rho}}=\sqrt{\frac{\lambda}{8}}V$	[20]
λ	$0.3164\ \mathrm{Re}^{-0.25}$	[20]
Re	$\frac{VD}{\nu}$	-

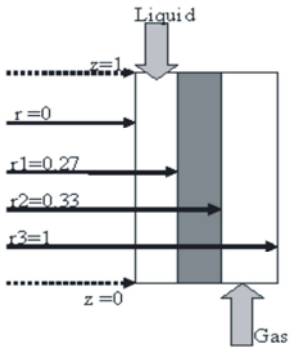

Fig. 2: Dimensionless schematic diagram of the membrane contactor

Numerical Solution: Physical properties for the gas mixture and liquid solvent are needed to solve the above set of equations at corresponding boundary conditions. These properties are listed in Table 2 and the dimensionless geometry is showed in Fig. 2. Where ε is the membrane porosity, τ is the membrane tortuosity, R is

Table 2: Dimensions of the membrane contactor and model parameters

Parameter	Value	Reference
Inner diameter of tube (mm)	1.52	[21]
Outer diameter of tube (mm)	1.83	[21]
Inner diameter of contactor (mm)	5.5	[21]
Total number of tubes	1	[21]
Contactor length (mm)	1190	[21]
$D_{CO_2-shell}(\mathrm{m}^2/\mathrm{s})$	1.855×10^{-5}[a]	[6]
$D_{CO_2-membrane}(\mathrm{m}^2/\mathrm{s})$	$D_{CO_2-shell}\ 3.71^{-6}$[b]	[6]
$D_{CO_2-tube}(\mathrm{m}^2/\mathrm{s})$	$2.35\times10^6 \exp(-2199/T)$	[6]
$D_{CO_2,turbulent-tube}(\mathrm{m}^2/\mathrm{s})$	$\frac{0.08}{Sc_{CO_2}^{T}}\times\frac{r1}{r3}\times\sqrt{\frac{0.3164\times\mathrm{Re}^{-.25}}{8}}\times V_{tube}$	[18, 20]
m (dimensionless)	$m=[2.82\times10^{-6}\exp(-2044/T)/(RT)]^{-1}$	[5]

[a]Calculated based on Chapman-Enskog theory which uses an equation for gas mixture with specific mole fractions.

[b]Effective diffusion coefficient is calculated considering the effects of porosity (0.4) and tortuosity (2.0) of the membrane, as provided by the membrane manufacturer

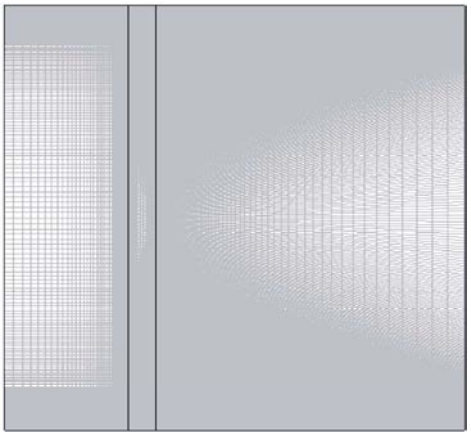

Fig. 3: Mapped meshing for the simulation of CO_2 capture in membrane contactor

the general gas constant and T is the temperature in Table 2. Initial concentration of CO_2 was considered 10% (v) at 25°C and 1 atm. The Reynolds number for the liquid flow was assumed 4500 for turbulent condition. Gas flow rate was considered 500 ml/min. Experiments were carried out for CO_2/CH_4 gas mixture using a tubular membrane contactor with PTFE membrane.

The model dimensionless equations with respect to tube, membrane and shell side with the appropriate boundary conditions were solved using COMSOL software, which uses finite element method, combined with mapped meshing (Fig. 3) and error control using a variety numerical solver such as UMFPACK [22]. This solver is an implicit time-stepping scheme, which is well suited for solving stiff and non-stiff non-linear boundary value problems.

RESULTS AND DISCUSSION

CO_2 Concentration Distribution for Turbulent Conditions

Concentration Gradient and Flux Vector of CO_2 in the Contactor: The representation of the concentration gradient and flux vector of CO_2 for turbulent flow conditions in the tube, membrane and shell side of the contactor is shown in Fig. 4. The gas mixture flows from one side of the contactor (Z=0) where the concentration of CO_2 is the highest (C_0), whereas the solvent flows from the other side (Z=L) where the concentration of CO_2 is assumed to be zero. As the gas flows through the shell side, it moves to the membrane side due to the concentration gradient and then is absorbed by the flowing solvent. For better understanding of problem the length of contactor is assumed to be 26 cm in this figure (22% of original contactor length which is 1.19 m)[21].

In both tube and shell compartments, the flux vector is in both r and z directions. Whereas it is only in r direction within the membrane. The flux vector at the tube side where solvent enters (Z = L) is the highest with higher r-directional flux at the gas-liquid interface, whereas, the effect of z-directional flux becomes more pronounced toward the tube center. Similar behavior is seen in the shell side.

Concentration Profile in Radial Direction: A sharp decrease in concentration can be seen in the tube side of the contactor, as presented in Fig. 5. It may be attributed to turbulent flow conditions. Another reason for such behavior is that diffusion coefficient in shell side is three

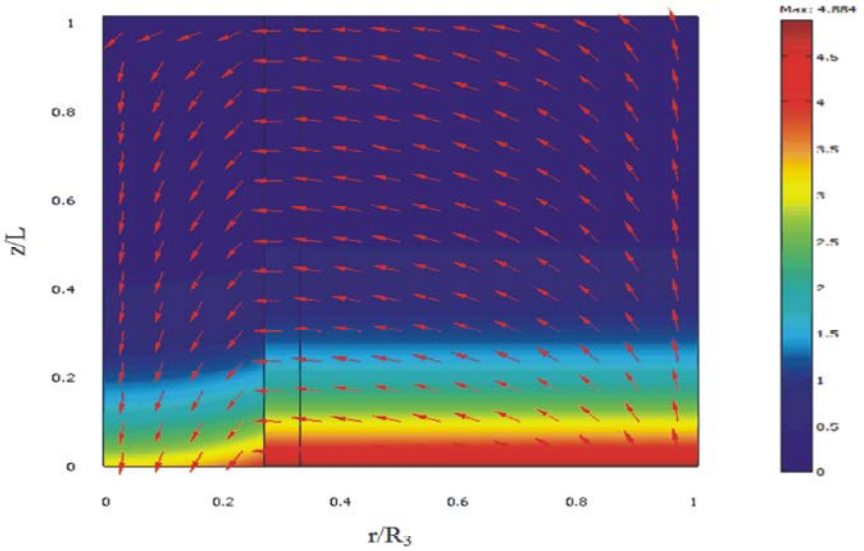

Fig. 4: Concentration gradient and flux vectors of CO_2 for turbulent liquid flow condition

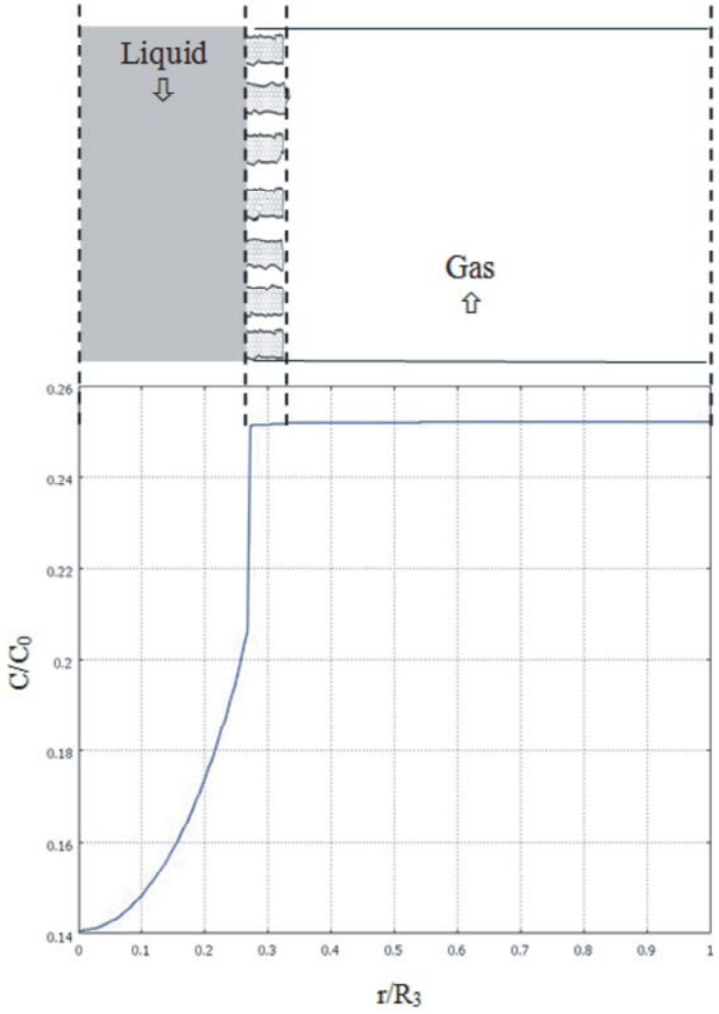

Fig. 5: CO_2 concentration in the radial direction of membrane contactor for turbulent liquid flow conditions at $Z/L = 0.2$

to four order of magnitude larger than it in the tube side. Thus, the resistance to CO_2 diffusion in the gas phase within the shell compartment is much smaller than it in the liquid phase flowing in the tube compartment. It is important to note that the concentration fraction (C/C_0) at $Z = L$ at the membrane-liquid interface is equivalent to that in the shell side since the resistance to CO_2 diffusion in the shell and membrane side is small compared to it in the tube side. Therefore, C can be considered as the average CO_2 concentration in the shell at z and C_0 is the inlet CO_2 concentration. Thus, the percentage removal of CO_2 can be calculated from the following equation:

$$\eta = 100\frac{Q_{in}\times C_{in} - Q_{out}\times C_{out}}{Q_{in}\times C_{in}} = 100(1-\frac{C_{out}}{C_{in}}) \qquad (19)$$

where Q_{in} and Q_{out} are the inlet and outlet gas volumetric flow rates (ml/min) and C_{in} and C_{out} are the inlet and outlet CO_2 volumetric concentrations in the gas phase (%), respectively and η is the CO_2 removal efficiency (%). Since the maximum CO_2 percent of the gas mixture at the inlet is 10, the change in gas volumetric flow rate is assumed to be negligible and thus % CO_2 removal can be approximated by Eq. (19). C_{out} is calculated using the following formula by means of COMSOL:

$$C_{out} = \frac{\int_{r_2}^{r_3} C(r,0)dr}{\int_{r_3}^{r_2} dr} \qquad (20)$$

Effect of Gas and Liquid Volumetric Flow Rates: The gas phase concentration and removal efficiency of CO_2 for turbulent flow condition along the length of the membrane contactor for different values of gas volumetric flow rates, which represent the effect of convection term, are presented in Figs. 6 and 7. As expected, the increase in the gas volumetric flow rate reduces the residence time of gas phase in the contactor, which in turn reduces the removal rate.

However, the convective term in the tube side has an opposite effect (Figs. 8 and 9). Increasing liquid volumetric flow rate increases the removal rate. As the solvent moves faster, the gas concentration at the inner surface of the tube along the contactor length becomes less, resulting in higher concentration gradient at the interface and thus CO_2 higher removal.

Effect of Initial CO_2 Concentration: Fig. 10 shows that the C/C_0 for CO_2 remains constant as the inlet concentration of CO_2 is increased. Because the outlet

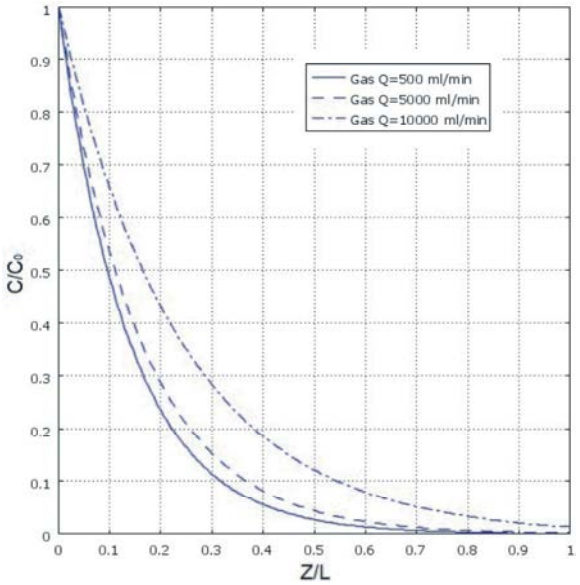

Fig. 6: Effect of gas volumetric flow rate on the average CO_2 concentration along the contactor length

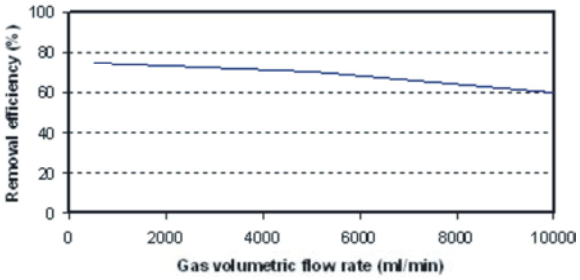

Fig. 7: Effect of gas volumetric flow rate on the removal efficiency of CO_2 at $Z/L = 0.2$

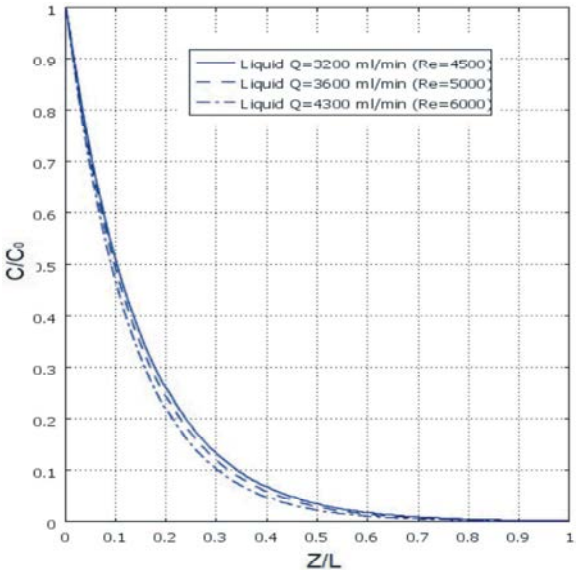

Fig. 8: Effect of liquid volumetric flow rate on the average CO_2 concentration along the contactor length

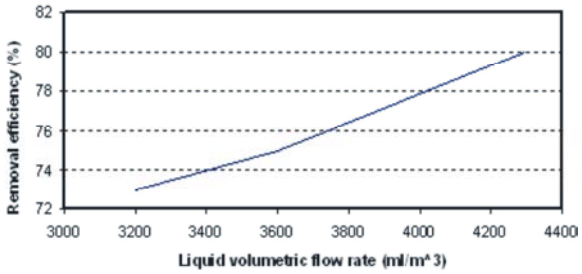

Fig. 9: Effect of liquid volumetric flow rate on the removal efficiency of CO_2 at $Z/L = 0.2$

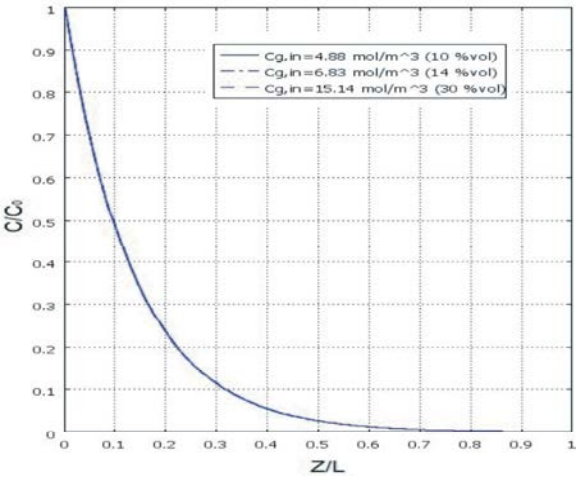

Fig. 10: Effect of initial CO_2 concentration on the average CO_2 concentration along the contactor length

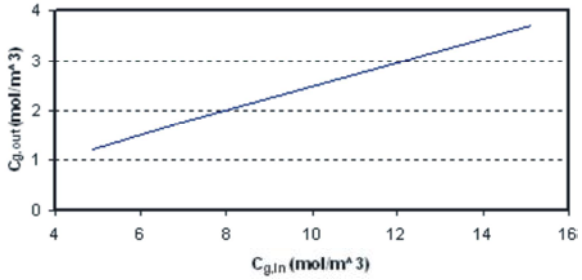

Fig. 11: Effect of inlet gas concentration on the outlet CO_2 concentration in the gas phase (physical absorption in water)

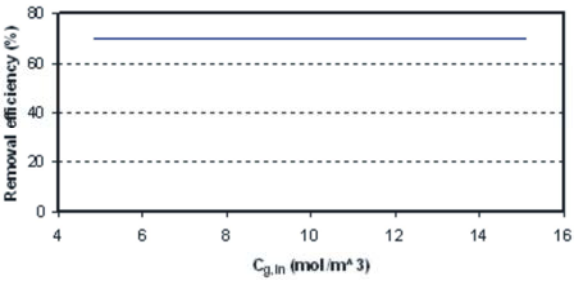

Fig. 12: Effect of inlet gas concentration on the removal efficiency of CO_2 at $Z/L = 0.2$

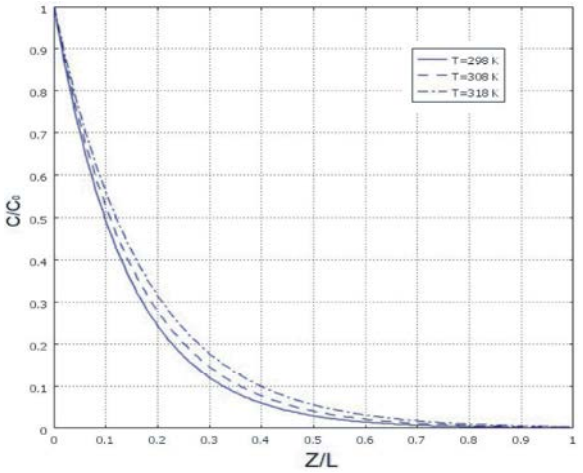

Fig. 13: Effect of temperature on the average CO_2 concentration along the contactor length

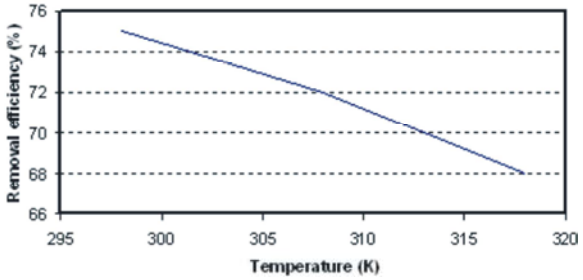

Fig. 14: Effect of temperature on the removal efficiency of CO_2 at $Z/L = 0.2$

CO_2 concentration in the gas phase is a function of the inlet concentration of CO_2. As the inlet concentration is increased, the outlet concentration is increased linearly (Fig. 11), So the absorbed CO_2 amount, which is described by the term (C_{in} - C_{out}), is increased with the same ratio resulting in constant removal rate according to Eq. 19 (Fig. 12).

Effect of Temperature: There is no reaction between water and CO_2 gas for converting CO_2 to other components, so the temperature effect on reaction rate has no importance in here. However, variation in temperature affects the physical solubility of CO_2 in water, which is approximated by m parameter. Increase in temperature increases the solubility of CO_2 in water. As concentration of gas increases at the inner side of the tube, it results in less concentration gradient at the interface and thus less CO_2 removal rate (Figs. 13, 14).

CO_2 Concentration Distribution for Laminar Conditions Concentration Gradient and Flux Vector of CO_2 in the Contactor: All conditions used for the laminar flow

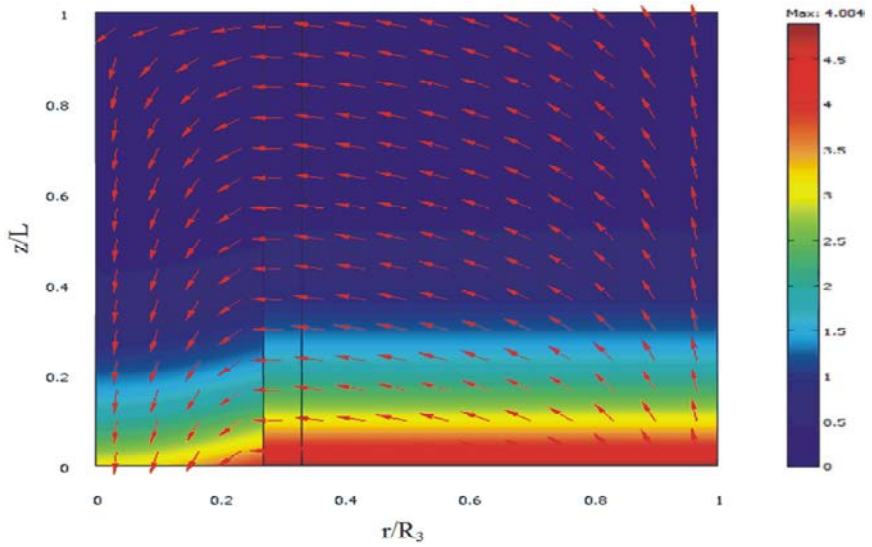

Fig. 15: Concentration gradient and flux vectors of CO_2 for laminar liquid flow condition

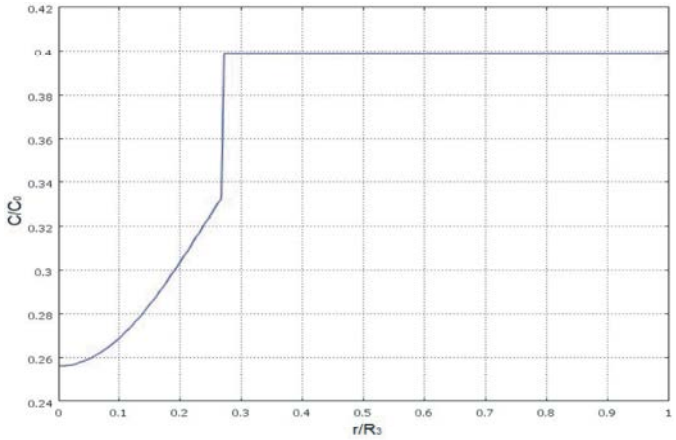

Fig. 16: CO_2 concentration in the radial direction of membrane contactor for laminar liquid flow conditions at $Z/L = 0.2$

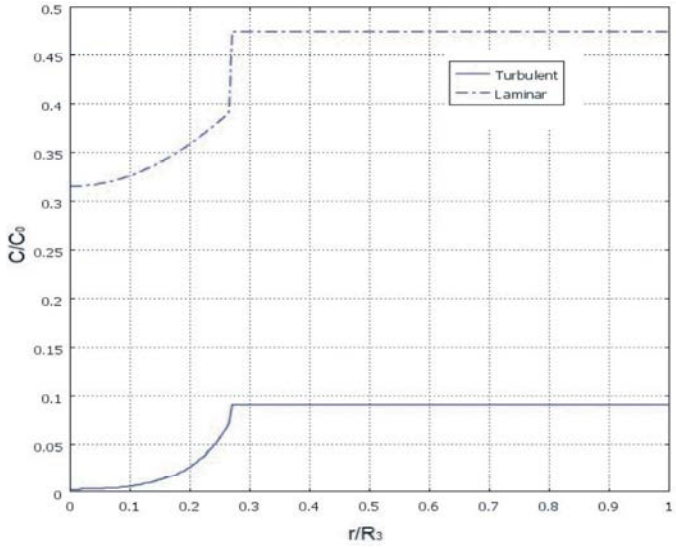

Fig. 17: CO_2 concentration in the radial direction at $Z/L = 0.2$

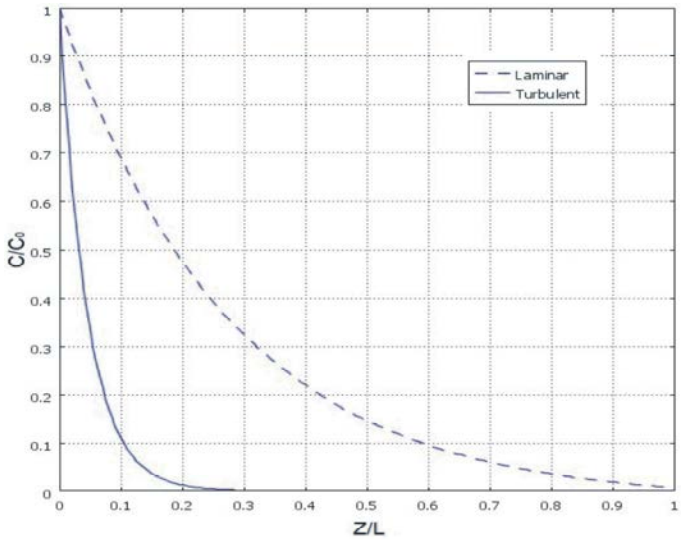

Fig. 18: Comparison of CO_2 concentration in Z direction of membrane contactor

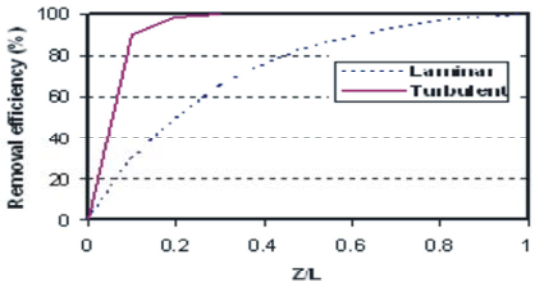

Fig. 19: Comparison of CO_2 removal efficiency in Z direction of membrane contactor

modeling for this analysis such as meshing data, contactor parameters, fluids physical properties, membrane and etc. were the same as the turbulent flow conditions. In addition, the operating temperature and pressure were set at 298K and 1 atm, respectively. However, three main differences were the liquid velocity (Re of liquid phase flow=500), equation of liquid velocity profile and diffusion coefficient in liquid phase which are used for this condition. The concentration gradient and flux vector of CO_2 are illustrated in Fig. 15 for laminar flow conditions. There is a concentration gradient pattern similar to Fig. 4, while in order to attain zero concentration at the outlet of the gas phase, the contactor has been presumed to be 119 cm in length, which made dimensionless afterwards.

Concentration Profile in Radial Direction: With respect to Fig. 16 increasing concentration in shell and membrane side is not sensible but it is decreased in tube side. This trend is almost similar to it for turbulent flow conditions.

Comparison of Absorption Process for Laminar and Turbulent Flows: Simulation results for laminar and turbulent flows are compared in Figs. 17 and 18. In Fig. 17, CO_2 concentration is shown in the radial direction at $Z/L = 0.2$ for laminar and turbulent flow conditions. Fig. 18 shows the variation of CO_2 concentration in Z direction of membrane contactor for laminar and turbulent flow conditions. As shown in these two figures, decreasing CO_2 concentration in turbulent flow condition is higher than it in laminar flow condition.

In each point along the dimensionless length of contactor, the removal efficiency in turbulent flow condition is higher than that of laminar flow condition (Fig. 19). Therefore, with operating in turbulent flow condition, higher removal efficiency can be obtained.

CONCLUSION

A mathematical model was developed to simulate the gas transport in tubular membrane contactors. The model was developed for non-wetting conditions, taking into consideration the diffusion in the tube, membrane and shell compartments of the contactor. The simulation results for the physical absorption of CO_2 in water indicated that the removal of CO_2 is increased with increasing liquid volumetric flow rate. On the other hand, increasing temperature and gas volumetric flow rate has an opposite effect. Increasing initial CO_2 concentration in inlet gas has no effect on the removal efficiency. Effective length for complete removal of CO_2 is 22% of original length for turbulent flow conditions, which means the contactor length can be 78% of the original size and it

leads to lower production costs due to less material involved. Comparison of some above results with the same results for laminar flow condition shows that the use of turbulent flow condition is better. Chemical reaction between gas and solvent, changing direction and position of fluids can be considered in future studies in this field.

REFERENCES

1. Gabelman, A. and S.T. Hwang, 1999. J. Membr. Sci., 159: 61.
2. Mansourizadeh, A. and A.F. Ismail, 2009. J. Hazard. Mater., 171: 38.
3. Zhang, H.Y., R. Wang, D. Tee Liang and J. Hwa Tay, 2006. J. Membr. Sci., 279: 301.
4. Al-Marzouqi, M., M.H. El-Naas, H. Muftah, S.A.M. Marzoukb, M.A. Al-Zarooni, N. Abdullatif and R. Faiz, 2008. Sep. Purif. Technol., 59: 286.
5. Al-Marzouqia, M., M.H. El-Naasa, S.A.M. Marzoukb and N. Abdullatif, 2008. Sep. Purif. Technol., 62: 501.
6. Keshavarz, P., J. Fathikalajahi and S. Ayatollahi, 2008 Sep. Purif. Technol., 63: 145.
7. Keshavarz, P., S. Ayatollahi and J. Fathikalajahi, 2008. J. Membr. Sci., 325: 98.
8. Shirazian, S., A. Moghadassi and S. Moradi, 2009. Simul. Model. Pract. Th., 17: 708.
9. Mohebi, S., S.M. Mousavi and S. Kiani, 2009. J. Nat. Gas. Chem., 1: 195.
10. Faiz, R. and M. Al-Marzouqi, 2009. J. Membr. Sci., 342: 269.
11. Faiz, R. and M. Al-Marzouqi, 2010. J. Membr. Sci., 350: 200.
12. Sohrabi, M.R., A. Marjani, S. Moradi, M. Davallo and S. Shirazian, 2011. Appl. Math. Model., 35: 174.
13. El-Naas, M.H., M. Al-Marzouqi, S.A. Marzouk and N. Abdullatif, 2010. J. Membr. Sci., 350: 410.
14. Eslami, S., S.M. Mousavi, S. Danesh and H. Banazadeh, 2011. Adv. Eng. Softw., 42: 73.
15. Grandison, A.S. and M.J. Lewis, 1996. Separation processes in the food and biotechnology industries, Woodhead Publishing, London.
16. Pellerin, E., E. Michelitsch, K. Darcovich, S. Lin and C.M. Tam, 1995. J. Membr. Sci., 100: 139.
17. Bird, R.B., W.E. Stewart and E.N. Lightfoot, *Transport phenomena*, John Wiley and Sons, New York.
18. Lorke, A. and F. Peeterse, 2006. J. Phys. Oceanogr., 36: 955.
19. Hasegawa, Y. and N. Kasagi, 2001. Proc 4th Int. Conf. on Multiphase Flow, New Orleans, USA. May 27 June 1.
20. Chowdury, S.H.J., 2007. J. Mech., pp: 38.
21. YeDouglas, X. and M. LeVan, 2003. J. Membr. Sci., 221: 147.
22. COMSOL multiphysics module users guide, COMSOL AB (2008).